Bifurcation Analysis of Cardiac Alternans Using δ-Decidability

Md. Ariful Islam[1(✉)], Greg Byrne[2], Soonho Kong[1], Edmund M. Clarke[1], Rance Cleaveland[3], Flavio H. Fenton[4], Radu Grosu[5,6], Paul L. Jones[2], and Scott A. Smolka[5]

[1] Carnegie Mellon University, Pittsburgh, PA, USA
mdarifui@cs.cmu.edu
[2] US Food and Drug Administration, Silver Spring, MD, USA
[3] University of Maryland, College Park, MD, USA
[4] Georgia Institute of Technology, Atlanta, GA, USA
[5] Vienna University of Technology, Vienna, Austria
[6] Stony Brook University, Stony Brook, NY, USA

Abstract. We present a bifurcation analysis of electrical alternans in the two-current Mitchell-Schaeffer (MS) cardiac-cell model using the theory of δ-decidability over the reals. Electrical alternans is a phenomenon characterized by a variation in the successive *Action Potential Durations* (APDs) generated by a single cardiac cell or tissue. Alternans are known to initiate re-entrant waves and are an important physiological indicator of an impending life-threatening arrhythmia such as ventricular fibrillation. The bifurcation analysis we perform determines, for each control parameter τ of the MS model, the *bifurcation point* in the range of τ such that a small perturbation to this value results in a transition from alternans to non-alternans behavior. To the best of our knowledge, our analysis represents the first formal verification of non-trivial dynamics in a numerical cardiac-cell model.

Our approach to this problem rests on encoding alternans-like behavior in the MS model as a 11-mode, multinomial hybrid automaton (HA). For each model parameter, we then apply a sophisticated, guided-search-based reachability analysis to this HA to estimate parameter ranges for both alternans and non-alternans behavior. The bifurcation point separates these two ranges, but with an uncertainty region due to the underlying δ-decision procedure. This uncertainty region, however, can be reduced by decreasing δ at the expense of increasing the model exploration time. Experimental results are provided that highlight the effectiveness of this method.

1 Introduction

An important component of cardiac electrodynamic modeling is the ability to understand and predict qualitative changes that take place in the dynamics as model parameters are varied [1,9,29]. One well-known change involves a transition to *alternans*: a phenomenon characterized by a period-doubling bifurcation where, while cells are paced at a constant period, their response has different

E. Bartocci et al. (Eds.): CMSB 2016, LNBI 9859, pp. 132–146, 2016.
DOI: 10.1007/978-3-319-45177-0_9

dynamics between even and odd beats, with one long action potential following a short one [23]. Alternans are known to destabilize waves [15] and initiate re-entrant waves and represent an important physiological indicator of an impending life-threatening arrhythmia such as ventricular fibrillation [19,27].

About 100 mathematical models [10] have been developed to recreate and study, to varying degrees of complexity, the electrical dynamics of a cardiac cell (i.e., cardiomyocyte). A particularly appealing one in terms of its mathematical tractability is the model of Mitchell and Schaeffer [24], which represents the cellular electrodynamics using only two state variables: a voltage variable v that describes the trans-membrane potential, and a gating variable h that describes the internal ionic state of the cell.

In this paper, we present a bifurcation analysis of electrical alternans in the two-current Mitchell-Schaeffer (MS) cardiac-cell model[1] using the theory of δ-decidability over the reals [12]. The bifurcation analysis we perform determines, for each parameter τ of the MS model, the *bifurcation point* in the range of τ such that a small perturbation to this value results in a transition from alternans to non-alternans behavior; see Fig. 1. To the best of our knowledge, our analysis represents the first formal verification of non-trivial dynamics in a realistic cardiac-cell model.

Our approach to this problem rests on encoding alternans-like behavior in the MS model as an 10-mode, multinomial hybrid automaton (HA). For each MS model parameter, we then apply a sophisticated, guided-search-based reachability analysis to this HA to estimate ranges for both alternans and non-alternans behavior. The bifurcation point separates these two ranges, but with an uncertainty region due to the underlying δ-decision procedure. This uncertainty region, however, can be reduced by decreasing δ at the expense of increasing the model exploration time. Experimental results are provided that highlight the effectiveness of this method.

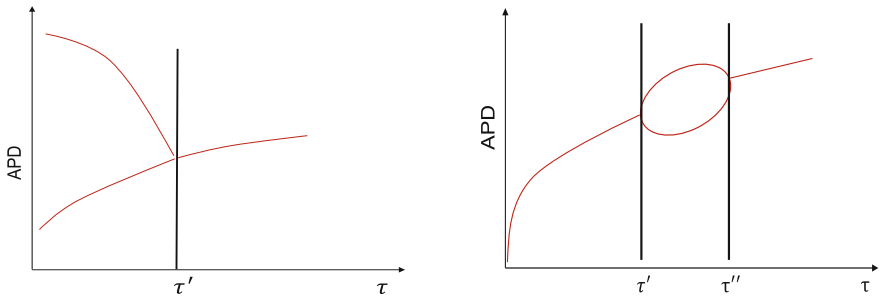

(a) Single period-doubling (b) Regular & reverse period-doubling

Fig. 1. Bifurcation analysis of *alternans* for parameter τ. Parameter values τ' and τ'' are bifurcation points.

[1] A third current I_s, which is not intrinsic to the MS model, is used to stimulate the cell to produce an action potential.

This paper is organized as follows. Section 2 presents the MS model and gives a brief overview of the dReach tool that we use to perform reachability analysis. Section 3 represents the MS model as an HA and then extends the MS HA to encode alternans behavior. Section 4 formally defines *bifurcation analysis* of alternans, and outlines an approach to perform the analysis by reducing it to a parameter-synthesis problem for the HA that encodes alternans. Section 5 presents our results for the bifurcation analysis of all of the control parameters of the MS model. Section 6 considers related work. Section 7 offers our concluding remarks and directions for future work.

2 Background

2.1 Mitchell-Schaefer Model

The Mitchell-Schaefer model is an activator-inhibitor system that describes the electrical dynamics of a ventricular myocyte. The model involves two coupled, nonlinear ordinary differential equations of the form:

$$\begin{aligned} \dot{v} &= I_{in}(v,h) + I_{out}(v) + I_s(t) \\ \dot{h} &= \begin{cases} \frac{1-h}{\tau_{open}} & v < V_g \\ \frac{-h}{\tau_{close}} & v \geq V_g \end{cases} \end{aligned} \tag{1}$$

where $v(t)$ is the transmembrane voltage and $h(t)$ is a gating variable (as in a voltage-gated ion channel [10]). The voltage ranges from -85 to 20 mV in a real cardiac cell, but has been scaled to the range $[0, 1]$ in the MS model, and is expressed as the sum of three currents: an inward current, outward current and stimulation current. The inward current $I_{in}(v,h) = hv^2(1-v)/\tau_{in}$ is designed to replicate the behavior of fast-acting gates found in more complex models. The outward current $I_{out}(v) = -v/\tau_{out}$ is ungated and represents the currents that act to decrease the membrane voltage. The strength of each respective current is controlled by the timing parameters τ_{in} and τ_{out}.

The stimulus current I_s is an externally applied current which is used to periodically excite an action potential in the cell. It is applied every BCL (Basic Cycle Length) milliseconds for a duration of τ_s milliseconds. The stimulation parameters used in this work are $[\tau_s, I_s]$=$[1, 0.2]$.

The gating variable $h(t)$ is dimensionless and scaled between 0 and 1. Parameters τ_{close} and τ_{open} are time constants that control the opening and closing of the h-gate, and V_g is the "critical" gating voltage; i.e., the voltage required to generate an action potential. The four time constants in the model are used to control the four phases of the cardiac action potential.

For certain parameter values, the Mitchell-Schaeffer model can exhibit alternans, a state which successively exhibits alternating short-long values of the APD. An example of alternans and non-alternans behavior in the voltage time series is shown in Fig. 2.

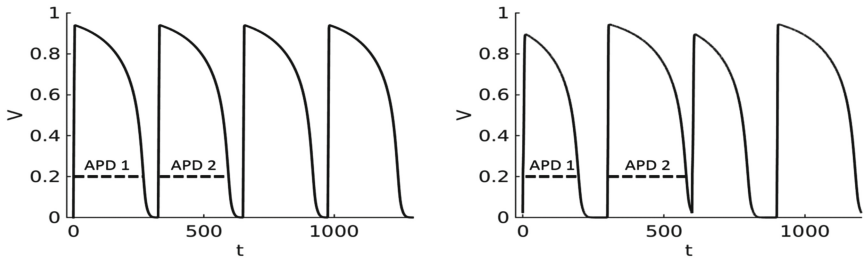

(a) BCL=325 (b) BCL=300

Fig. 2. The voltage time series for the Mitchell-Schaeffer model using parameter values $[\tau_{in}, \tau_{out}, \tau_{open}, \tau_{close}, V_g]$=$[0.3, 6, 20, 150, 0.1]$. The threshold value used to compute the APD is $V_T = 0.2$. (a) The time series does not meet the definition of alternans since APD1=APD2. (b) The time series meets the definition of alternans since the APDs alternate in length (short, long, short long).

2.2 The dReach Tool

dReach [21] is a bounded reachability analysis tool for nonlinear hybrid systems. It takes a hybrid automaton $\mathcal{H}$, reachability properties $\mathcal{P}$, a numerical error bound $\delta \in \mathbb{Q}^+$, and an unrolling depth $k \in \mathbb{N}$ as inputs. It then encodes a bounded-reachability problem for a hybrid automaton as a first-order formula over the reals and solves the formula using the delta-decision SMT solver dReal [14]. There are two possible outputs from the dReach tool:

- unreachable: dReach confirms that there is no trace satisfying the reachability properties up to k discrete jumps.
- δ-reachable: dReach shows that there exists a trace ξ satisfying the reachability properties if we consider a user-specified numerical perturbation $\delta \in \mathbb{Q}^+$ in $\mathcal{H}$. The tool also provides a feature to visualize this trace.

We note that the bounded-reachability problem for nonlinear hybrid automata is undecidable [3]. The tool is implemented in the framework of delta-complete analysis for bounded reachability of hybrid systems [13], which provides an algorithm for the originally undecidable problem by using approximation (the use of δ in the analysis).

3 Hybrid Automata for the MS Model and Alternans

In this section, we represent the MS model as a hybrid automaton and extend this automaton to encode alternans and non-alternans behavior.

3.1 Hybrid Automaton ($\mathcal{H}_M$) for the MS model

The stimulus current $I_s(t)$ in Eq. 1 is typically a periodic square-wave pulse of fixed duration (τ_s). An example of such a wave form is shown in Fig. 3.

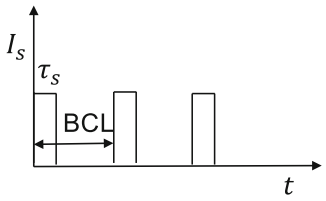

Fig. 3. A typical wave form for the stimulus current $I_s(t)$ with period=BCL and stimulus duration $= \tau_s$.

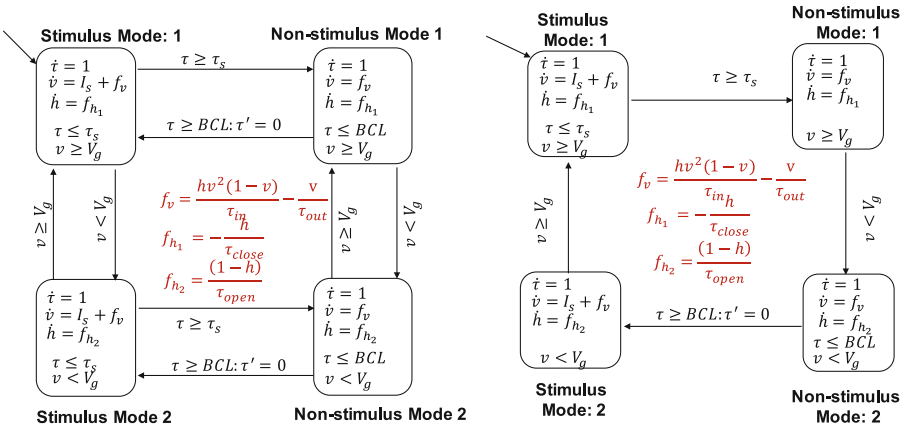

(a) Detailed MS Automaton (b) Simplified MS Automaton $\mathcal{H}_M$

Fig. 4. The four-mode hybrid automaton for the MS model. The primed version of variables is used to indicate the reset map of a given transition. Variables not shown in the reset map are not updated during the jump.

To handle this type of stimulus signal in the MS model, we split the voltage dynamics into two separate modes: a stimulus mode and a non-stimulus mode.

Since the dynamics of variable h is also separable into two modes, we can represent the MS cardiac-cell model as a four-mode hybrid automaton (HA) whose schematic is shown in Fig. 4(a). We add an additional state variable τ that serves as a local clock for time-triggered events; for example, the transition from a stimulus to a non-stimulus mode or the transition from the current AP cycle to the next.

Due to the following observations, we can simplify this HA by removing certain edges:

- $v < V_g$ will not occur in "Stimulation Mode 1", as the value of v always increases in this mode
- $v \ge V_g$ will not occur in "Non-stimulation Mode 2", as v always decreases in this mode

– $v \geq V_g$ occurs before $\tau \geq \tau_s$ in "Stimulus Mode 2"
– For a chosen BCL range, $v < V_g$ occurs before $\tau \geq BCL$ in "Non-stimulus Mode 1"

3.2 Encoding Alternans and Non-Alternans as Hybrid Automata

We now encode a modified definition of alternans that incorporates transient cycles and a tolerance threshold r_{th}, $0 \leq r_{th} \leq 1$, which establishes the relative difference between APDs. Transients are important since, when starting from an initial state and a set of parameters that are known to produce alternans, the voltage signal only settles into period-doubling after the transient phase is over. Failure to incorporate transient cycles can result in unwanted effects on the alternans calculation. We add the tolerance threshold r_{th} to take into account noise and measurement errors in the clinical data that is used to calculate alternans.

Definition 1. *Let σ be a (possibly infinite) voltage signal that begins with N_{trans} AP cycles, followed by at least two AP cycles, where N_{trans} is the number of transient cycles. Let $\tau_1 > 0$ and $\tau_2 > 0$ be the APDs of any two consecutive AP cycles after the initial N_{trans} cycles in σ. Further, let $r = \frac{\tau_2}{\tau_1}$. We say that σ* exhibits alternans with respect to a given r_{th} *when $|r - 1| > r_{th}$ is an invariant. Likewise, we say that σ* exhibits non-alternans with respect to r_{th} *when $|r - 1| \leq r_{th}$ is an invariant.*

As opposed to using the absolute value of the difference of consecutive APDs ($|APD_1 - APD_2|$) for the definition of alternans, Definition 1 yields a *normalized* (between 0 and 1) basis for comparison. Note that as r_{th} is increased, the estimated bifurcation point is moved away from the exact value and farther into the alternans region. In the limit as r_{th} approaches zero, the estimated bifurcation point approaches the exact value, as shown in Fig. 5.

We first explain the steps used to encode alternans as an HA based on $\mathcal{H}_M$, and then follow similar steps to encode non-alternans as another HA. We consider alternans as a safety property and characterize it using a so-called *safety automaton* [2]. For our purposes, a safety automaton is an HA with modes additionally marked as *accepting* or *non-accepting*, and with the property that no

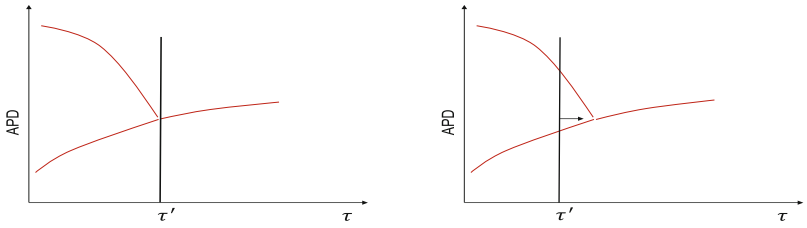

(a) $r_{th} = 0$ (b) $r_{th} \neq 0$

Fig. 5. Effect of r_{th} on bifurcation point.

accepting mode can be reaching from a non-accepting mode. After first determining that $\mathcal{H}_M$ has completed N_{trans} transient cycles, our safety, or *observer*, automaton $\mathcal{H}_O$ repeatedly computes two successive APDs τ_1 and τ_2, and checks if the condition for alternans (Definition 1) is violated. If so, the automaton enters a trap (i.e. non-accepting) state, from which it never exits. If no such violation is detected, then the observed sequence of cycles is accepted. Thus, in $\mathcal{H}_O$, there is a single non-accepting mode named "Trap"; all other modes are accepting. Note that $\mathcal{H}_O$ uses the v and τ values from $\mathcal{H}_M$ to determine when a cycle has completed and to compute APD values.

Figure 6 presents observer HA $\mathcal{H}_O$ for the alternans problem. As, by definition, APD is the time period in each AP cycle during which $v \geq V_T$, an APD event can occur only in "Stimulus Mode: 1" and "Non-stimulus Mode: 1" in $\mathcal{H}_M$. So to compute APD, the observer splits "Non-stimulus Mode: 1" into two modes: "APD Mode" (when $v \geq V_T$) and "Non-APD Mode" (when $v < V_T$). As the "Stimulus Mode: 1" is at most τ_s and τ_s (typically 1 ms) is negligible compared to the duration of "Non-stimulus Mode: 1" (> 200 ms), we ignore the event $v \geq V_T$ inside "Stimulus Mode: 1" for the APD computation. This helps us avoid splitting "Stimulus Mode: 1" and thus reduces the number of modes in the observer HA.

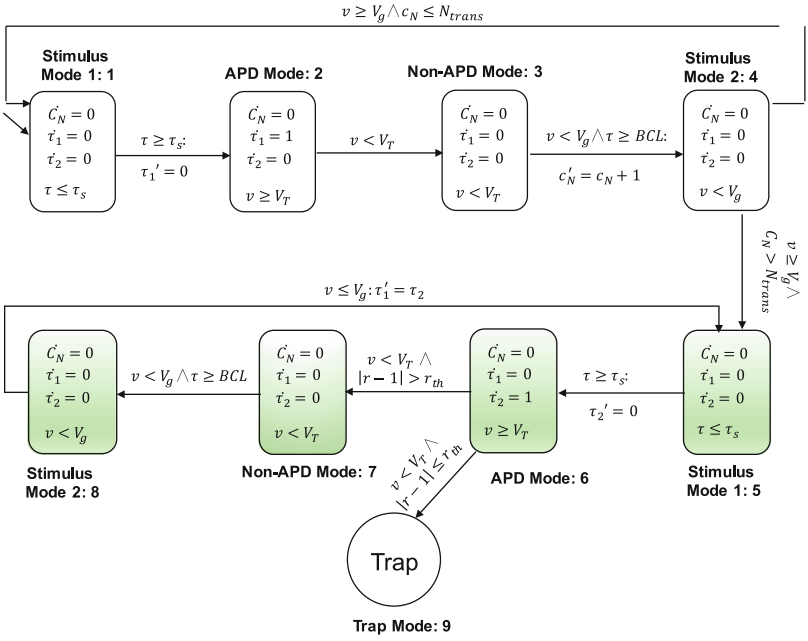

Fig. 6. The hybrid automaton $\mathcal{H}_O$ for the observer. The number after the colon in each mode name gives a number to the mode. Mode "Trap" is non-accepting; all other modes are accepting.

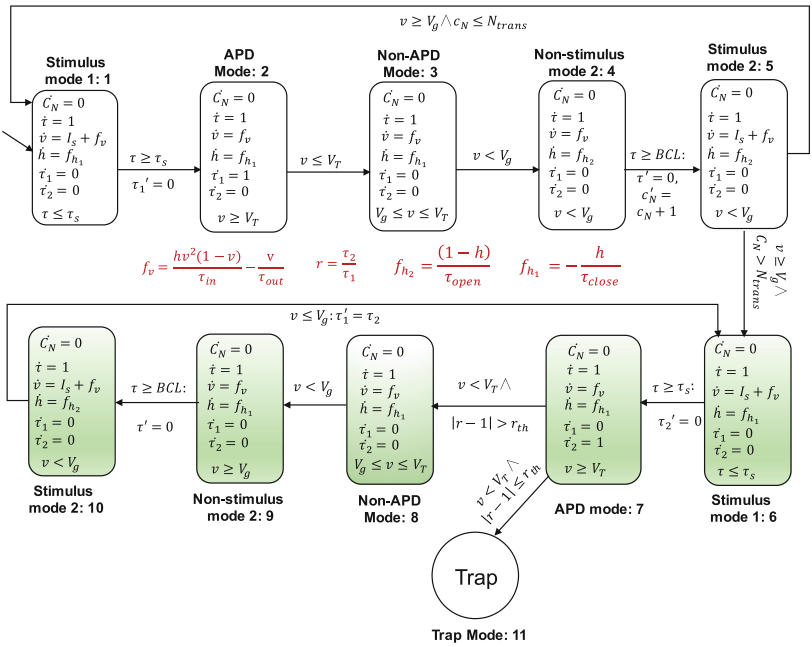

Fig. 7. The 11-mode hybrid automaton $\mathcal{H}_A$ for alternans.

To determine whether $\mathcal{H}_M$ completes N_{trans} transient cycles, we add a counter C_N in $\mathcal{H}_O$ which is increased by 1 during the jump from "Non-APD Mode: 3" to "Stimulus Mode 2: ". In $(N_{trans}+1)$ cycle, $\mathcal{H}_O$ computes τ_1 in "APD Mode: 2" and then compute τ_2 in the consequent cycle in "APD Mode: 6". When $v < V_T \wedge |r-1| > r_{th}$ does not hold, a transition from"APD Mode: 6" to "Trap Mode: 9" occurs, i.e., the alternans property is violated. All the other modes are the accepting states for this safety (Buechi) automaton.

To check the alternans property, we combine $\mathcal{H}_M$ and $\mathcal{H}_O$ into a single automaton $\mathcal{H}_A$ as shown in Fig. 7. This approach is known as shared-variable composition [4].

Let Θ_0 be a set of initial states in $\mathcal{H}_O$. We say Θ_0 produce alternans when:

$$\exists \theta_0 \in \Theta_0. \text{“Trap Mode: 11” is not reachable in } \mathcal{H}_A. \tag{2}$$

Similar to Fig. 7, we can encode the dual behavior, non-alternans, as an HA $\mathcal{H}_N$ by inter-changing guard conditions of the outgoing transitions in "APD Mode: 7". We then say that that Θ_0, a set of initial states in $\mathcal{H}_N$, produces non-alternans when:

$$\exists \theta_0 \in \Theta_0. \text{“Trap Mode: 11” is not reachable in } \mathcal{H}_N. \tag{3}$$

4 Bifurcation Analysis of Alternans Using dReach

To perform bifurcation analysis of alternans for a parameter τ of the MS model, we need to augment the state vector of both $\mathcal{H}_A$ and $\mathcal{H}_N$ with τ by adding $\dot{\tau} = 0$ in each mode. Let $R_\tau = [\underline{\tau}, \overline{\tau}]$ be the set of initial values of τ. Now we define the set of initial states of both augmented automata as $\Theta_0^a = \theta_0 \times R_\tau$, where θ_0 is some nominal initial state from where both $\mathcal{H}_A$ and $\mathcal{H}_N$ start operating.

Now we will redefine the problem (2) and (3) based on the augmented automata. Let Θ_0^a be a set of initial states in the augmented automata. We say Θ_0^a produce alternans, when

$$\exists \theta_0^a \in \Theta_0^a. \text{ “Trap Mode: 11” is not reachable in augmented } \mathcal{H}_A. \tag{4}$$

Algorithm 1. Bifurcation Analysis on dReach

```
1: procedure BIFURCATION-ANALYSIS(τ,R_τ,δ_0)
2:     add τ̇ = 0 in H_A and H_N
3:     AR ← {}   NR ← {}   UR ← R_τ   δ ← δ_0
4:     while UR meets desired precision criteria do
5:         UR ← RECURSIVESEARCH(δ, UR)
6:         Decrease δ
7:     end while
8: end procedure
```

Similarly, we say Θ_0^a produce non-alternans, when

$$\exists \theta_0^a \in \Theta_0^a. \text{ “Trap Mode: 11” is not reachable in augmented } \mathcal{H}_N. \tag{5}$$

Algorithm 1 serves as an outline of our bifurcation analysis of alternans, for τ varying in range R_τ, using dReach-based reachability analysis on problems (4) and (5). The algorithm will partition R_τ into three regions: 1) *Alternans Region* (AR), 2) *Non-alternans Region* (NR) and 3) *Uncertainty Region* (UR) which contains the bifurcation point (BP).

Algorithm 1 starts by augmenting $\mathcal{H}_\mathcal{A}$ and $\mathcal{H}_N$ with τ and initializing AR, NR, UR and δ. In the while-loop, it then calls a recursive search procedure to reduce the size of the UR, while concomitantly computing AR and NR. The algorithm terminate when size of the UR meets the desired precision criteria (i.e., the UR is small enough).

In the recursive search procedure, we first initialize Θ_0^a, which we will use for both automata. We then run dReach on problem (4). If dReach returns *unsat* for this problem, we add UR to NR and return the empty set for the new UR. If it returns δ-*sat*, however, we run dReach on the dual problem as shown on line 8. If dReach returns *unsat* for the dual problem, we add UR to AR and return the empty set for the new UR.

In both cases, when dReach returns δ-*sat* and the size of UR becomes less than or equal to current δ, we return UR as the new uncertainty region as

```
1: procedure RecursiveSearch(UR,δ)
2:     Θ_0^a = θ_0 × UR
3:     α ← dReach(H_A, Θ_0^a, δ)
4:     if α = unsat then
5:         NR ← NR ∪ UR
6:         return {}
7:     end if
8:     β ← dReach(H_N, Θ_0^a, δ)
9:     if β = unsat then
10:        AR ← AR ∪ UR
11:        return {}
12:    end if
13:    if |UR| ≤ δ then
14:        return UR
15:    end if
16:    (UR^l, UR^r) ← Bisect(UR)
17:    return RecursiveSearch(UR^l, δ) ∪ RecursiveSearch(UR^r, δ)
18: end procedure
```

shown on line 14. If, however, the size of UR is greater than δ, we bisect UR and recursively call the search method on both branches, returning their union as the new UR.

Figure 8 provides an example of our bifurcation analysis of alternans. Figure 8(a) shows the exact bifurcation analysis that we wish to achieve using δ-decidability over the reals. Figure 8(b) shows the bifurcation analysis using Algorithm 1. Initially, the entire range is considered as an UR in Algorithm 1. The algorithm then iteratively reduces UR and increases AR and NR. Figure 8(c), shows how the recursive search procedure, in a binary-search-tree-like fashion, computes AR and NR and reduces UR.

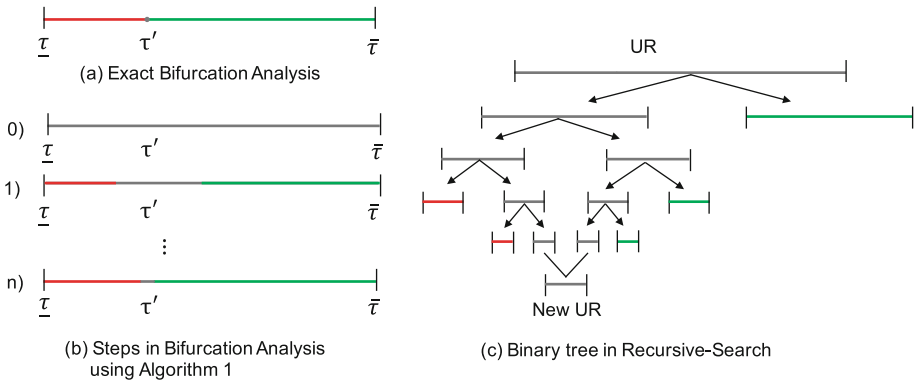

Fig. 8. Bifurcation analysis of alternans. Red: AR, Green: NR, Gray: UR. (Color figure online)

5 Results

In this section, we present the results of performing *bifurcation analysis* of alternans over five parameters in the MS model using Algorithm 1. When we perform bifurcation analysis for a parameter, we fix the other parameter as follows:

$[V_g, r_{th}, N_{trans}, BCL, \tau_{in}, \tau_{out}, \tau_{open}, \tau_{close}]$ are set to $[0.1, 0.2, 2, 300, 0.3, 6, 20, 150]$ unless specified otherwise. The fixed initial condition θ_0 for $\mathcal{H}_A$ and $\mathcal{H}_N$ were taken as $v(0) = 0.2$, $h(0) = 1$ with $C_N(0)$, $\tau(0)$, $\tau_1(0)$ and $\tau_2(0)$ all set to zero. In all cases, we consider voltage signal that contains $N_{trans} + 2$ AP cycles.

For the *bifurcation analysis* of *alternans* for *BCL*, we consider the range as $[300, 330]$, $\delta_0 = 0.5$. We perform the bifurcation analysis for three different r_{th} values. Figure 9, for three different r_{th},illustrates the partitioning of the range of *BCL* into three regions: *AR*, *NR* and *UR* and Table 1 shows the corresponding subranges computed by Algorithm 1. We also overlay the simulation-based *bifurcation diagram* to help visualizing the position of the *bifurcation point*. The sequence of figures illustrate how the bifurcation region returned by dReach approaches the exact bifurcation point as r_{th} approaches zero.

We summarize the *bifurcation analysis* for other parameters in Table 2 for $r_{th} = 0.01$ and Fig. 10 shows their bifurcation diagrams. Note that we are not able to find any BP for τ_{open}. All computation is performed using Intel Core i7-4770 CPU @ 3.40 GHz $\times$ 8 on Linux platform.

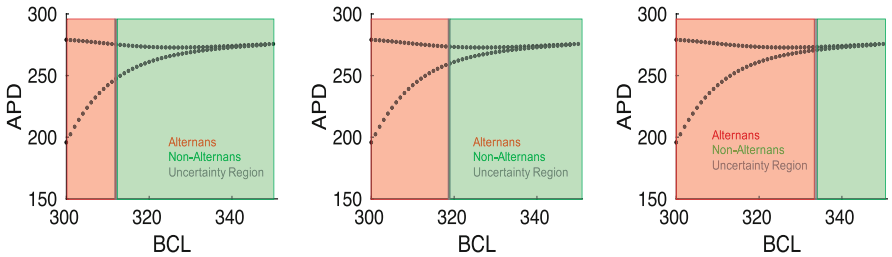

(a) $r_{th} = 0.1$ (b) $r_{th} = 0.05$ (c) $r_{th} = 0.01$

Fig. 9. *Bifurcation analysis* of *alternans* with respect to BCL for three different r_{th} values.

Table 1. Parameter ranges for *alternans* and *non-alternans* and uncertainty region.

r_{th}	*AR*	*NR*	*UR*	Runtime (s)
0.1	$[300, 311.91]$	$[311.912, 350]$	$(311.91, 311.912)$	80, 209
0.05	$[300, 318.564]$	$[318.567, 350]$	$(318.564, 318.567)$	81, 012
0.01	$[300, 332.4714]$	$[332.4716, 330]$	$(332.4714, 332.4716)$	81, 162

Table 2. Parameter ranges for *alternans* and *non-alternans* and uncertainty region.

Parameter	*AR*	*NR*	*UR*	Runtime (s)
τ_{in}	$[0.3, 0.3729]$	$[0.3730, 0.4]$	$(0.3729, 0.3720)$	176010
τ_{out}	$[4.9995, 6]$	$[3, 4.9990]$	$(4.9990, 4.9995)$	66000
τ_{open}	$[7.5, 20]$	–	–	110231
τ_{close}	$[131.8586, 150]$	$[130, 131.8584]$	$(131.8584, 131.8586)$	84938

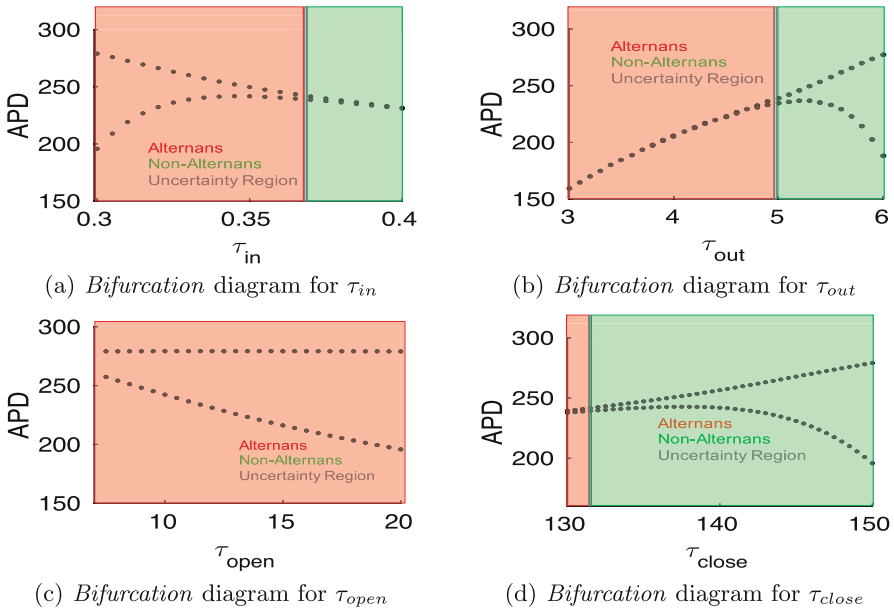

(a) *Bifurcation* diagram for τ_{in}

(b) *Bifurcation* diagram for τ_{out}

(c) *Bifurcation* diagram for τ_{open}

(d) *Bifurcation* diagram for τ_{close}

Fig. 10. *Bifurcation analysis* of *alternans* with respect to four parameters of the MS model with $r_{th} = 0.01$.

6 Related Work

Reachability analysis has emerged as a promising solution for many biological systems [6,11,17,31]. SMT-based verification using dReal [14] has been applied in various problems [5,8,18,20,25,26]. Liu et al. successfully applied SMT-based reachability analysis using dReach in identifying patient-specific androgen ablation therapy schedules for postponing the potential cancer relapse in [22].

Brim et al. present a bifurcation analysis technique to analyze stability of genetic regulatory networks in [7]. They first express various stability-related properties by a temporal logic language extended by directional propositions and then verify those properties by varying the model parameters. Even though they apply their method only on piece-wise affine dynamics, the authors claim that it can be extended for piece-wise multiaffine dynamics. The method, however, is not applicable for general nonlinear dynamical systems.

In [16], Huang et al. presents a reachability analysis technique for a hybrid model of cardiac dynamics for a 1-d cable of cells and show the presence of alternans based on computed reachtube. The authors, however, neither define nor verify the alternans property formally. They just do reachability analysis for two *BCL* values and show, by visual inspection, that one *BCL* value produces alternans and another does not.

7 Conclusions

In this paper, we have applied reachabilty analysis to identify the bifurcation points that represent the transition to alternans in the Mitchell-Schaefer cardiac-cell model. Our bifurcation analysis is performed using the bounded-reachability tool dReach [21], and uses a sophisticated guided-search strategy to"zoom in" on the bifurcation point in question. Since this tool is designed to work with nonlinear hybrid systems, we converted the original MS model into a hybrid automaton (HA), and further extended this HA to encode alternans- and non-alternans-like behavior.

For future work, we intend to study other models where alternans are not due to solely the voltage dynamics, as in the MS model. Rather, they may also be caused by the calcium dynamics, as both mechanisms have been found to occur in cardiac cells [28]. Such models can have multiple BPs and our algorithm will automatically find all of them, as it searches for BPs in each branch of the recursive search tree.

We also plan to extend the cell-level bifurcation analysis we conducted to a 1-d cable of cells. Traveling waves can exhibit alternans along cables [30]. Doing so, will require us to extend our reachability analysis from ODEs to PDEs. We can also extend our analysis by varying multiple parameters simultaneously; currently, we only vary one parameter at a time. We can accomplish this by augmenting the state vector with each of these parameters.

Acknowledgments. We would like to thank the anonymous reviewers for their helpful comments. Research supported in part by the following grants: NSF IIS-1447549, NSF CPS-1446832, NSF CPS-1446725, NSF CNS-1446665, NSF CPS 1446365, NSF CAR 1054247, AFOSR FA9550-14-1-0261, AFOSR YIP FA9550-12-1-0336, CCF-0926190, ONR N00014-13-1-0090, and NASA NNX12AN15H.

References

1. Shrier, A., Dubarsky, H., Rosengarten, M., Guevara, M.R., Nattel, S., Glass, L.: Prediction of complex atrioventricular conduction rhythms in humans with use of the atrioventricular nodal recovery curve. Circulation **76**(6), 1196–1205 (1987)
2. Alpern, B., Schneider, F.B.: Recognizing safety and liveness. Distrib. Comput. **2**(3), 117–126 (1987)
3. Alur, R., Courcoubetis, C., Henzinger, T.A., Ho, P.: Hybrid automata: an algorithmic approach to the specification and verification of hybrid systems. In: Hybrid Systems, pp. 209–229 (1992)

4. Alur, R., Henzinger, T.A., Ho, P.-H.: Automatic symbolic verification of embedded systems. IEEE Trans. Softw. Eng. **22**(3), 181–201 (1996)
5. Bae, K., Ölveczky, P.C., Kong, S., Gao, S., Clarke, E.M.: SMT-based analysis of virtually synchronous distributed hybrid systems. In: Proceedings of the 19th International Conference on Hybrid Systems: Computation and Control, pp. 145–154. ACM (2016)
6. Batt, G., De Jong, H., Page, M., Geiselmann, J.: Symbolic reachability analysis of genetic regulatory networks using discrete abstractions. Automatica **44**(4), 982–989 (2008)
7. Brim, L., Demko, M., Pastva, S., Šafránek, D.: High-performance discrete bifurcation analysis for piecewise-affine dynamical systems. In: Abate, A., et al. (eds.) HSB 2015. LNCS, vol. 9271, pp. 58–74. Springer, Heidelberg (2015). doi:10.1007/978-3-319-26916-0_4
8. Bryce, D., Gao, S., Musliner, D.J., Goldman, R.P.: SMT-based nonlinear PDDL+ planning. In: 29th AAAI Conference on Artificial Intelligence, p. 3247
9. Fenton, F.H., Cherry, E.M., Hastings, H.M., Harold, M., Evans, S.J.: Multiple mechanisms of spiral wave breakup in a model of cardiac electrical activity. chaos: an interdisciplinary. J. Nonlinear Sci. **12**(3), 852 (2002)
10. Fenton, F.H., Cherry, E.M.: Models of cardiac cell. Scholarpedia **3**(8), 1868 (2008)
11. Feret, J.: Reachability analysis of biological signalling pathways by abstract interpretation. In: Computation in Modern Science and Engineering, vol. 2, Part A (AIP Conference Proceedings vol. 963), pp. 619–622 (2007)
12. Gao, S., Avigad, J., Clarke, E.M.: δ-complete decision procedures for satisfiability over the reals. In: Gramlich, B., Miller, D., Sattler, U. (eds.) IJCAR 2012. LNCS, vol. 7364, pp. 286–300. Springer, Heidelberg (2012)
13. Gao, S., Kong, S., Chen, W., Clarke, E.M.: Delta-complete analysis for bounded reachability of hybrid systems. CoRR, abs/1404.7171 (2014)
14. Gao, S., Kong, S., Clarke, E.M.: dReal: an smt solver for nonlinear theories over the reals. In: Bonacina, M.P. (ed.) CADE 2013. LNCS, vol. 7898, pp. 208–214. Springer, Heidelberg (2013)
15. Gizzi, A., Cherry, E.M., Gilmour, R.F., Luther, S., Filippi, S., Fenton, F.H.: Effects of pacing site and stimulation history on alternans dynamics and the development of complex spatiotemporal patterns in cardiac tissue. Front. Physiol. **4**, 71 (2013)
16. Huang, Z., Fan, C., Mereacre, A., Mitra, S., Kwiatkowska, M.: Invariant verification of nonlinear hybrid automata networks of cardiac cells. In: Biere, A., Bloem, R. (eds.) CAV 2014. LNCS, vol. 8559, pp. 373–390. Springer, Heidelberg (2014)
17. Islam, M.A., De Francisco, R., Fan, C., Grosu, R., Mitra, S., Smolka, S.A.: Model checking tap withdrawal in C. Elegans. In: Hybrid Systems Biology, p. 195
18. Islam, M.A., Murthy, A., Girard, A., Smolka, S.A., Grosu, R.: Compositionality results for cardiac cell dynamics. In: Proceedings of the 17th international conference on Hybrid systems: computation and control, pp. 243–252. ACM (2014)
19. Weiss, J.N., Alain, S., Shiferaw, Y., Chen, P., Garfinkel, A., Qu, Z.: From pulsus to pulseless the saga of cardiac alternans. Circ. Res. **98**(10), 1244–1253 (2006). WOS: 000237812200006
20. Kapinski, J., Deshmukh, J.V., Sankaranarayanan, S., Arechiga, N.: Simulation-guided Lyapunov analysis for hybrid dynamical systems. In: Hybrid Systems: Computation and Control (HSCC), pp. 133–142. ACM Press (2014)
21. Kong, S., Gao, S., Chen, W., Clarke, E.M.: dReach: δ-reachability analysis for hybrid systems. In: Proceedings of Tools and Algorithms for the Construction and Analysis of Systems - 21st International Conference, TACAS, London, UK, April 11–18, 2015, pp. 200–205 (2015)

22. Liu, B., Kong, S., Gao, S., Zuliani, P., Clarke, E.M.: Towards personalized prostate cancer therapy using delta-reachability analysis. In: Proceedings of the 18th International Conference on Hybrid Systems: Computation and Control, pp. 227–232. ACM (2015)
23. Guevara, M., Glass, L., Shrier, A.: Phase locking, period-doubling bifurcations, and irregular dynamics in periodically stimulated cardiac cells. Science **214**(4527), 1350–1353 (1981)
24. Mitchell, C.C., Schaeffer, D.G.: A two-current model for the dynamics of cardiac membrane. Bull. Math. Biol. **65**(5), 767–793 (2003)
25. Murthy, A., Islam, M.A., Smolka, S.A., Grosu, R.: Computing bisimulation functions using SOS optimization and δ-decidability over the reals. In: Proceedings of the 18th International Conference on Hybrid Systems: Computation and Control, pp. 78–87. ACM (2015)
26. Murthy, A., Islam, M.A., Smolka, S.A., Grosu, R.: Computing compositional proofs of input-to-output stability using SOS optimization and δ-decidability. Hybrid Systems, Nonlinear Analysis (2016)
27. Gilmour, R.F., Chialvo, D.R.: Electrical restitution, critical mass, and the riddle of fibrillation. J. Cardiovas. Electrophysiol. **10**(8), 1087–1089 (1999)
28. Shiferaw, Y., Sato, D., Karma, A.: Coupled dynamics of voltage and calcium in paced cardiac cells. Phys. Rev. E **71**(2), 021903 (2005)
29. Quail, T., Shrier, A., Glass, L.: Predicting the onset of period-doubling bifurcations in noisy cardiac systems. Proc. Nat. Acad. Sci. **112**(30), 9358–9363 (2015)
30. Watanabe, M.A., Fenton, F.H., Evans, S.J., Hastings, H.M., Karma, A.: Mechanisms for discordant alternans. J. Cardiovasc. Electrophysiol. **12**(2), 196–206 (2001)
31. Yang, Y., Lin, H.: Reachability analysis based model validation in systems biology. In: 2010 IEEE Conference on Cybernetics and Intelligent Systems (CIS), pp. 14–19. IEEE (2010)